I R A M P
10(1), June 2019, pp. 31-37

© International Science Press
ISSN: 2229-39-44

Single and Double Ionization of Helium by Collisions with H^+, He^{2+}, and Li^{3+}

M. S. PINDZOLA[1] AND T.G. LEE[2]

[1]Department of Physics, Auburn University, Auburn, AL
[2]U.S. Naval Research Laboratory, Washington, D.C., USA

ABSTRACT: The time-dependent close-coupling method is used to calculate cross sections for the single and double ionization of He in collisions with H+ and He2+ ions at 400 keV/amu, and Li3+ ions at 390 keV/amu. Two electron transitions are taken into account. The results are checked against the cross-beam experimental data and good agreement is found.

1. INTRODUCTION

Ionization involving two active electrons remains of considerable theoretical and experimental interest primarily due to the fact that electron-electron correlation can play a dominant role in the process. The simplest process for which the correlated-electron dynamic can be studied is single photon double ionization of helium. Ionization of a helium atom induced by ion impact is more challenging owing to two-center Coulomb interactions between the projectile and the target [1] Nevertheless, over the years respectable theoretical and some experimental efforts have been put forward to understand the ionization dynamics of this basic four-body breakup system. Recent experimental work focusing on energy and angular distribution of the ejected electrons in ionization of He by fast ion impact were reported in Gassert *et al* [2] and Biswas *et al* [3].

Over the years, the non-perturbative time-dependent close coupling (TDCC) method has been developed and successfully applied to treat inelastic collisions processes in a variety of ion-atom and ion-molecule collisions [4, 5]. Recently, the TDCC method was applied to investigate single and double ionization of He by 1.0 - 1.6 MeV/amu α-particle impact. It is shown that the TDCC calculated results [6] are in good agreement with results obtained from other close coupling calculations [7] and experiments for total cross sections [8, 9]. For single and double ionization of He by C^{6+} ions at 100 MeV/amu, the TDCC results [10] were able to provide some insights on the discrepancies between theory and experiment [11]. The TDCC method has been extended to examine single and double ionization cross sections for U^{92+} + He at 1 GeV/amu collisions. The results [12] were compared with experimental data [13] and very good agreement is achieved. The TDCC method has been applied to calculate neutron projectile induced single and double ionization of He atom at incident energies between 10 keV and 200 keV. The results [14] for cross section ratio of double to single ionization are found to be in reasonable agreement with the calculations based on exterior complex scaling method [15]. For single and double ionization of He by F^{9+} ions at 4 MeV/amu, the one active electron TDCC results [16] appeared to yield a better agreement with the experiment [17] for single ionization cross section. More recently, the TDCC method has been developed and applied to investigate energy-dependent excitation cross sections of the Na atom by proton impact. Cross sections for $3s \rightarrow \{nl\}$ excitations of the Na atom were calculated for proton-impact energies ranging from 1.0 to 100.0 keV [18]. It is found that the TDCC calculated cross sections agree with the atomic orbital close-coupling calculations [19] across the energy range, whereas the experimental cross sections [20] are slightly above the theoretical cross sections over most of the energy range.

In this paper we present the single, single with excitation, and double ionization cross sections of He by impact with H^+ and He^{2+} ions at 400 keV/amu and Li^{3+} ions at 390 keV/amu based on the TDCC method. The non-perturbative method allows us to incorporate the interaction of two continuum electrons in the presence of a positive

ion field in an accurate manner. The accuracy of the cross section results from TDCC calculations is assessed by comparing against the available experimental cross sections.

The rest of the paper is organized as follows: we review the theoretical formulation of the time-dependent close-coupling methods in Section 2, calculations and cross section results for the single, single with excitation, and double ionization of He by H^+, He^{2+}, and Li^{3+} ions are presented in Section 3. Finally, a summary is given in Section 4. Unless otherwise stated, all quantities are given in atomic units.

2. THEORY

In previous work the time-dependent close-coupling method was developed for the fast bare ion-impact ionization of He [6]. For ionization of the Helium atom with two active electrons by a fast bare ion, the total electronic wavefunction may be expanded in terms of radial wavefunctions, $P^{LM}_{l_1 l_2}(r_1, r_2, t)$, and coupled spherical harmonics. Upon substitution into the time-dependent Schrodinger equation, we obtain the time-dependent close-coupling equations given by:

$$i\,\frac{\partial P^{LM}_{l_1 l_2}(r_1,r_2,t)}{\partial t} = \sum_{i=1,2} T_{l_i}(r_i) P^{LM}_{l_1 l_2}(r_1,r_2,t) + \sum_{l_1',l_2'} V^{L}_{l_1,l_2,l_1',l_2'}(r_1,r_2) P^{LM}_{l_1' l_2'}(r_1,r_2,t) + \sum_{L',M'} \sum_{l_1',l_2'} \sum_{i=1,2} W^{LM,L'M'}_{l_1 l_2, l_1' l_2'}\left(r_i, R_p(t)\right) P^{L'M'}_{l_1' l_2'}(r_1,r_2,t) \qquad (1)$$

The kinetic and nuclear operator is given by:

$$T_l(r) = -\frac{1}{2}\frac{\partial^2}{\partial r^2} + \frac{l(l+1)}{2r^2} - \frac{Z_t}{r} \qquad (2)$$

where $Z_t = 2$ for He. The Coulomb repulsion operator is given by:

$$V^{L}_{l_1 l_2, l_1' l_2'}(r_1,r_2) = (-1)^{L+l_2+l_2'} \sqrt{(2l_1+1)(2l_1'+1)(2l_2+1)(2l_2'+1)} \times \sum_{\lambda} \frac{(r_1,r_2)^{\lambda}_{<}}{(r_1,r_2)^{\lambda+1}_{>}} \begin{pmatrix} l_1 & \lambda & l_1' \\ 0 & 0 & 0 \end{pmatrix} \begin{pmatrix} l_2 & \lambda & l_2' \\ 0 & 0 & 0 \end{pmatrix} \begin{Bmatrix} L & l_2' & l_1' \\ \lambda & l_1 & l_2 \end{Bmatrix} \qquad (3)$$

The fast bare ion operators are given by:

$$W^{LM,L'M'}_{l_1 l_2, l_1' l_2'}\left(r_1, R_p(t)\right) = -Z_p \delta_{l_2,l_2'} (-1)^{l_2+L+L'-M} \times \sqrt{(2l_1+1)(2l_1'+1)(2L+1)(2L'+1)} \times \sum_{\lambda} (-1)^{\lambda} \frac{\left(r_1, R_p(t)\right)^{\lambda}_{<}}{\left(r_1, R_p(t)\right)^{\lambda+1}_{>}} \begin{pmatrix} l_1 & \lambda & l_1' \\ 0 & 0 & 0 \end{pmatrix} \begin{Bmatrix} l_1 & l_2 & L \\ L' & \lambda & l_1' \end{Bmatrix} \times \sum_{q} C^{\lambda *}_{q}(\theta_p, \phi_p) \begin{pmatrix} L & \lambda & L' \\ -M & q & M' \end{pmatrix} \qquad (4)$$

$$W^{LM,L'M'}_{l_1 l_2, l_1' l_2'}\left(r_2, R_p(t)\right) = -Z_p \delta_{l_1,l_1'} (-1)^{l_1+l_2-l_2'-M} \times \sqrt{(2l_2+1)(2l_2'+1)(2L+1)(2L'+1)} \times \sum_{\lambda} (-1)^{\lambda} \frac{\left(r_2, R_p(t)\right)^{\lambda}_{<}}{\left(r_2, R_p(t)\right)^{\lambda+1}_{>}} \begin{pmatrix} l_2 & \lambda & l_2' \\ 0 & 0 & 0 \end{pmatrix} \begin{Bmatrix} l_2 & l_1 & L \\ L' & \lambda & l_2' \end{Bmatrix} \times \sum_{q} C_q^{\lambda *}(\theta_p, \phi_p) \begin{pmatrix} L & \lambda & L' \\ -M & q & M' \end{pmatrix} \tag{5}$$

where $Z_p = 1, 2, 3$ for H^+, He^{2+}, Li^{3+}.The time-dependent projectile position is given by:

$$R(t) = \sqrt{b^2 + (d_0 + vt)^2} \tag{6}$$

where b is an impact parameter, d_0 is a starting distance, and v is the projectile speed. A set of bound, $P_{nl}(r)$, radial orbitals are determined by the diagonalization of the Hamiltonian of Eq.(2).

The initial condition for the solution of Eq.(1) is given by:

$$P^{LM}_{l_1,l_2}(r_1, r_2, t=0) = \sum_{l_1',l_2'} \bar{P}^{L_0M_0}_{l_1'l_2'}(r_1, r_2) \delta_{l_1,l_1'} \delta_{l_2,l_2'} \delta_{L,L_0} \delta_{M,M_0}, \tag{7}$$

where the radial wavefunctions, $\bar{P}^{L_0M_0}_{l_1'l_2'}(r_1, r_2)$, are obtained by relaxation of Eq.(1) in imaginary time without the fast bare ion operators. Asymptotic radial wavefunctions, $\bar{P}^{LM}_{l_1'l_2'}(r_1, r_2, t \to \infty)$, are obtained by time propagating Eq.(1) in real time including the fast bare ion operators until the projectile has moved well past the target.

For the $l_1 l_2 L_0 M_0$ channels:

$$P^{L_0M_0}_{l_1,l_2}(r_1, r_2) = P^{L_0M_0}_{l_1,l_2}(r_1, r_2, t \to \infty) - O_{lap} \bar{P}^{L_0M_0}_{l_1 l_2}(r_1, r_2) \tag{8}$$

and for all other $l_1 l_2 LM$ channels:

$$P^{L_0M_0}_{l_1,l_2}(r_1, r_2) = P^{LM}_{l_1,l_2}(r_1, r_2, t \to \infty), \tag{9}$$

where the overlap factor is given by:

$$O_{lap} = \sum_{l_1,l_2} \int_0^{\infty} dr_1 \int_0^{\infty} dr_2 \, \overline{\bar{P}^{L_0M_0}_{l_1,l_2}}(r_1, r_2) P^{L_0M_0}_{l_1,l_2}(r_1, r_2, t \to \infty). \tag{10}$$

The total single ionization probability, for a given velocity and impact parameter, is given by:

$$P_{sion}(v,b) = \sum_{l_1,l_2,L,M} \sum_{n} \Big(\int_0^{\infty} dr_2 \Big| \int_0^{\infty} dr_1 \, P_{nl_1}(r_1) \, P^{LM}_{l_1,l_2}(r_1, r_2) \Big|^2 - \sum_{n'} \Big| \int_0^{\infty} dr_1 \int_0^{\infty} dr_2 \, P_{nl_1}(r_1) P_{n'l_2}(r_2) P^{LM}_{l_1,l_2}(r_1, r_2) \Big|^2 + \int_0^{\infty} dr_1 \Big| \int_0^{\infty} dr_2 \, P_{nl_2}(r_2) P^{LM}_{l_1,l_2}(r_1, r_2) \Big|^2$$

$$-\sum_{n'} |\int_0^\infty dr_1 \int_0^\infty dr_2 \; P_{n'l_1}(r_1) P_{nl_2}(r_2) P^{LM}_{l_1,l_2}(r_1,r_2)|^2) \tag{11}$$

The total double ionization probability, for a given velocity and impact parameter, is given by:

$$\begin{aligned} P_{dion}(v,b) = & \sum_{l_1,l_2,L,M} \int_0^\infty dr_1 \int_0^\infty dr_2 \, | P^{LM}_{l_1,l_2}(r_1,r_2)|^2 \\ -P_{sion}(v,b) - & \sum_{l_1,l_2,L,M} \sum_n \sum_{n'} |\int_0^\infty dr_1 \int_0^\infty dr_2 \, P_{nl_1}(r_1) P_{n'l_2}(r_2) P^{LM}_{l_1,l_2}(r_1,r_2)|^2 . \end{aligned} \tag{12}$$

For both single and double ionization, the total cross section is given by:

$$\sigma(v) = 2\,\pi \int_0^\infty P(v,b) b \, db. \tag{13}$$

3. RESULTS

The time-dependent close-coupling method was then used to calculate single and double ionization cross sections in H^+ + He and He^{2+} + He collisions at 400 keV/amu and Li^{3+} + He collisions at 390 keV/amu. For a 360 point uniform radial mesh with $\Delta r = 0.20$, diagonalization of the radial Hamiltonian of Eqs.(2) and (3) yields a set of He^+ bound radial orbitals. On a 360 $\times$ 360 point uniform radial mesh with $\Delta r_1 = \Delta r_2 = 0.20$, relaxation of Eq.(1) in imaginary time, without the fast bare ion operators, is carried out starting from a product of radial orbitals, $P_{1s}(r_1)P_{1s}(r_2)$, from the diagonalization and using the first 4 $l_1 l_2 LM$ coupled channels given in Table 1. Time propagation of Eq.(1) was made for all 101 close-coupled channels given in Table 1. The time propagation of Eq.(1) is made from $d_{initial} = -100$ to $d_{final} = +201$ at 40 impact parameters ranging from $b = 0.1$ to $b = 20.0$. The fast bare operators of Eqs.(4) and (5) included up to $\lambda = 3$ for the spherical tensors.

Table 1: TDCC coupled channels

	l_1	l_2	L	M		l_1	l_2	L	M		l_1	l_2	L	M
1	0	0	0	0	2	1	1	0	0	3	2	2	0	0
4	3	3	0	0	5	0	1	1	1	6	1	0	1	1
7	0	1	1	0	8	1	0	1	0	9	0	1	1	-1
10	1	0	1	-1	11	0	2	2	2	12	2	0	2	2
13	0	2	2	1	14	2	0	2	1	15	0	2	2	0
16	2	0	2	2	17	0	2	2	-1	18	2	0	2	-1
19	0	2	2	-2	20	2	0	2	-2	21	0	3	3	3
22	3	0	3	3	23	0	3	3	2	24	3	0	3	2
25	0	3	3	1	26	3	0	3	1	27	0	3	3	0
28	3	0	3	0	29	0	3	3	-1	30	3	0	3	-1
31	0	3	3	-2	32	3	0	3	-2	33	0	3	3	-3
34	3	0	3	-3	35	1	1	1	1	36	1	1	1	0
37	1	1	1	-1	38	1	1	2	2	39	1	1	2	1
40	1	1	2	0	41	1	1	2	-1	42	1	1	2	-2
43	2	2	1	1	44	2	2	1	0	45	2	2	1	-1
46	2	2	2	2	47	2	2	2	1	48	2	2	2	0
49	2	2	2	-1	50	2	2	2	-2	51	2	2	3	3
52	2	2	3	2	53	2	2	3	1	54	2	2	3	0
55	2	2	3	-1	56	2	2	3	-2	57	2	2	3	-3
58	1	2	1	1	59	2	1	1	1	60	1	2	1	0
61	2	1	1	0	62	1	2	1	-1	63	2	1	1	-1
64	1	2	2	2	65	2	1	2	2	66	1	2	2	1
67	2	1	2	1	68	1	2	2	0	69	2	1	2	0
70	1	2	2	-1	71	2	1	2	-1	72	1	2	2	-2

73	2	1	2	-2	74	1	2	3	3	75	2	1	3	3
76	1	2	3	2	77	2	1	3	2	78	1	2	3	1
79	2	1	3	1	80	1	2	3	0	81	2	1	3	0
82	1	2	3	-1	83	2	1	3	-1	84	1	2	3	-2
85	2	1	3	-2	86	1	2	3	-3	87	2	1	3	-3
88	1	3	3	3	89	3	1	3	3	90	1	3	3	2
91	3	1	3	2	92	1	3	3	1	93	3	1	3	1
94	1	3	3	0	95	3	1	3	0	96	1	3	3	-1
97	3	1	3	-1	98	1	3	3	-2	99	3	1	3	-2
100	1	3	3	-3	101	3	1	3	-3					

Table 2 shows the measured single, double ionization cross sections and double to single ionization cross-section ratios, respectively, together with the results of our TDCC calculations. Note that the Sommerfeld parameters for and 1 are 2.25, 0.5 and 0.25, respectively. This parameter measures the strength of the projectile field. For 0.5, non-perturbative theory is a more appropriate approach to the problem.

Table 2: Collision cross sections (Mb); σ_s: single ionization leaving $He^+(1s)$, σ_{s+ex}: single ionization leaving $He^+(nl)$ and σ_d: double ionization. The subscript "expt." denotes the experimental values of [9]. Ratio $R_{(th,expt)} = \sigma_d/\sigma_s$ are the theoretical and measured values (in 10^{-2}) (1.0 Mb = 1.0 $\times$ 10^{-18} cm^2)

Z_p	E(keV/amu)	σ_s	σ_{s+ex}	$\sigma_{s,expt}$	σ_d	$\sigma_{d,expt}$	R_{th}	R_{expt}
3	390	291	313	297$\pm$6	12.4	12.6$\pm$0.4	3.96	4.23$\pm$0.12
2	400	149	155	151.4$\pm$2.1	2.99	3.11$\pm$0.11	1.93	2.05$\pm$0.08
1	400	41.2	41.9	44.1$\pm$0.9	0.32	0.24$\pm$0.01	0.76	0.54 $\pm$ 0.03

The single ionization weighted probabilities as a function of impact parameter are shown in Figure 1. As it allows us to see which is the most important range of impact parameters for the total cross sections, we find that the single ionization probabilities peak at an impact parameter of approximately 1.0 for H^+ increasing to approximately 1.5 for Li^{3+}. In other words, the peak shifts to higher values of impact parameter as the projectile charge increases, suggesting that the emission is produced at larger impact parameters due to the stronger field of the projectile. Furthermore, large impact parameters region corresponds to small energy transfer to the target electron.

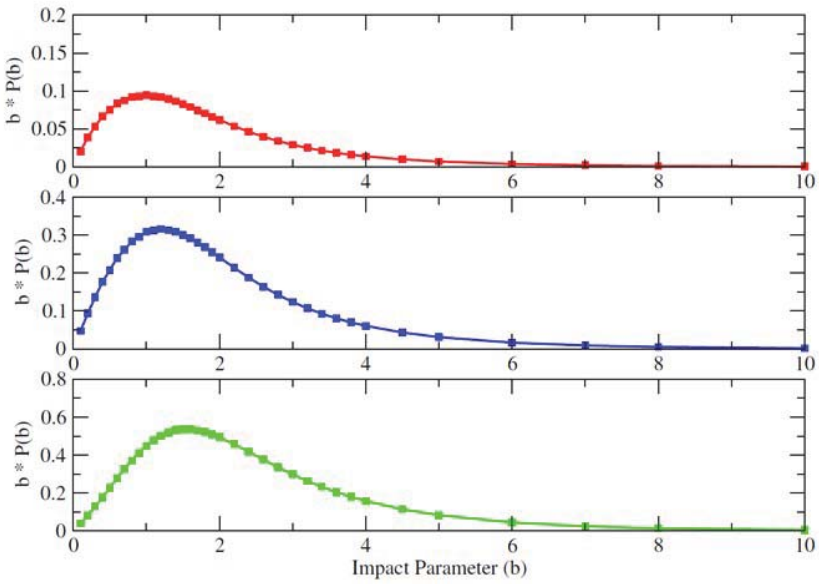

Figure 1. (color inline) Weighted probabilities for single ionization. Top graph: solid line with squares (red): H^+ + He collisions, middle graph: solid line with squares (blue): He^{2+} + He collisions, bottom graph: solid line with squares (green): Li^{3+} + He collisions.

The double ionization weighted probabilities as a function of impact parameter are shown in Figure 2. We see that the double ionization probabilities peak at an impact parameter of approximated 0.5 for H^+ increasing only

slightly for the other two ions as opposed to the single ionization. We can also see that double ionization requires smaller impact parameters, as already noted by Salin [21] at impact energy of 1.4 MeV/amu.

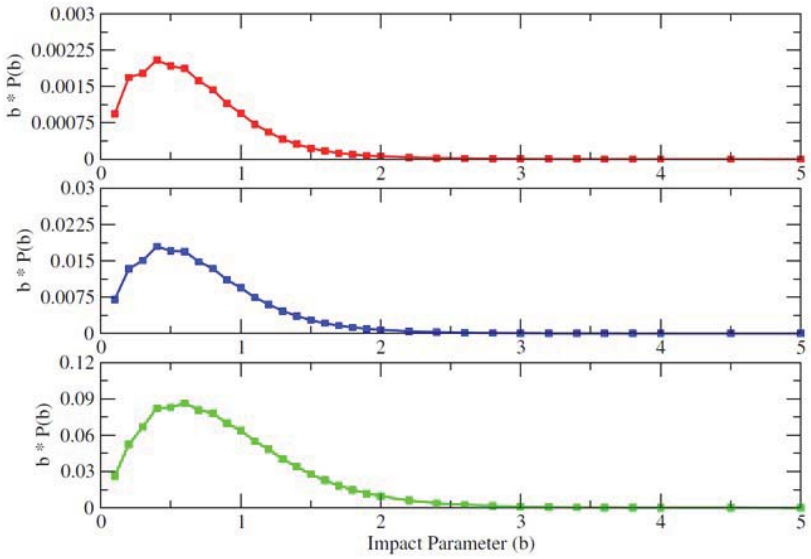

Figure 2. ***(color inline)*** **Weighted probabilities for double ionization. Top graph: solid line with squares (red): H^+ + He collisions, middle graph: solid line with squares (blue): He^{2+} + He collisions, bottom graph: solid line with squares (green): Li^{3+} + He collisions.**

4. SUMMARY

In summary, we have applied the time-dependent close-coupling method to calculate single and double ionization cross sections for H^+ + He and He^{2+} + He collisions at 400 keV/amu and Li^{3+} + He collisions at 390 keV/amu. In comparison to the experimental cross sections of Shah and Gilbody [9] we found that the TDCC method able to reproduce the experimental cross sections for single and double ionization of helium. We hope that the present calculations will stimulate further single and double ionization cross section measurements. In the future we plan to calculate single and double ionization cross sections for other bare ion collisions with He to identify trends as a function of impact energies.

Acknowledgments

This work was supported in part by grants from the US Department of Energy and the US National Science Foundation. Computational work was carried out at the National Energy Research Scientific Computing Center in Berkeley, California.

References

[1] Ovchinnikov S Yu, Ogurtsov G N, Macek J H and Gordeev Yu S 2004 Phys. Rep. **389** 119

[2] Gassert H, Chuluunbaatar O *et al* 2016 Phys. Rev. Lett. **116** 073201

[3] Biswas S, Misra D, Monti J M, Tachino C A, Rivarola R D, Tribedi L C 2014 Phys. Rev. A **90** 052714

[4] Pindzola M S et al 2007 J. Phys. B: At. Mol. Opt. Phys. **40** R39

[5] Pindzola M S, Colgan J, Robicheaux F, Lee T-G., Ciappina M F, Foster M, Ludlow J A and Abdel-Naby S A 2016 Adv. At. Mol. Opt. Phys. **65** 291

[6] Pindzola M S, Robicheaux F and Colgan J 2007 J. Phys. B: At. Mol. Opt. Phys. **40** 1695

[7] Barna I F, Grun N and Scheid W 2003 Eur. Phys. J. D **25** 239

[8] Knudsen H, Andersen L H, Hvelplund P, Astner G, Cederquist H, Danared H, Liljeby L and Rensfelt K G 1984 J. Phys. B: At. Mol.

Phys. **17** 3545

[9] Shah M B and Gilbody H B 1985 J. Phys. B: At. Mol. Phys. **18** 899

[10] Pindzola M S, Robicheaux F and Colgan J 2010 Phys. Rev. A **82** 042719

[11] Schulz M, Moshammer R, Fischer D, Kollmus H, Madison D H, Jones S and Ullrich J 2003 Nature **422** 48

[12] Ciappina M F, Pindzola M S and Colgan J 2013 J. Phys. B: At. Mol. Phys. **46** 215206

[13] Moshammer R *et al* 1997 Phys. Rev. Lett. **79** 3621

[14] Pindzola M S, Lee T G, Abdel-Naby Sh A, Robicheaux F, Colgan J and Ciappina M F 2014 J. Phys. B: At. Mol. Opt. Phys. **47** 195202

[15] Liertzer M, Feist J, Nagele S and Burgdorfer J 2012 Phys. Rev. Lett. **109** 013201

[16] Pindzola M S, Lee TG and Colgan J 2015 J. Phys. B: At. Mol. Opt. Phys. **48** 144019

[17] Misra D, Kelkar A H, Fainstein P D and Tribedi L C 2012 J. Phys. B: At. Mol. Opt. Phys. **45** 225201

[18] Pindzola M S and Loch S D 2019 J. Phys. B: At. Mol. Opt. Phys. **52** 025202

[19] Shingal R and Bransden B H 1987 J. Phys. B: At. Mol. Opt. Phys. **20** 4815

[20] Allen J S, Anderson L W and Lin C C 1988 Phys. Rev. A **37** 349

[21] Salin A 1987 Phys. Rev. A **36** 5471